Compact Modeling of GaN HEMT Based on Device-Internal Potential Distribution

Y. Okada, Y. Tanimoto, T. Mizoguchi, H. Zenitani, H. Kikuchihara, H. J. Mattausch, M. Miura-Mattausch
Graduate School of Advanced Sciences of Matter, Hiroshima University, Higashi-Hiroshima, Japan
E-mail: m154867@hiroshima-u.ac.jp

***Abstract*—A compact model of GaN HEMT is developed, which solves the Poisson equations explicitly. The model includes all possible charges induced within the device including the trap density. It is verified that the model can reproduce all 2D-device simulation results accurately. In particular, the operation frequency dependence of the current collapse can also be captured accurately by adjusting the trap time constant.**

Keywords—GaN; 2-dimentional electron gas; HEMT; compact model; surface potential;

I. INTRODUCTION

An important advantage of the GaN HEMT structure is its wide bandgap with additionally high carrier mobility. It is therefore utilized both for high voltage and at the same time for high speed applications [1,2]. The primary origin of the high performance of a GaN HEMT is the 2-dimensional electron gas (2DEG), induced at the AlGaN/GaN interface due to the band-edge mismatch between AlGaN and GaN. The 2DEG composes an inherent channel inversion charge which can be modified by applying the gate voltage (see Fig. 1). However, the AlGaN layer between the gate insulator and the channel in the GaN layer weakens the gate control and also induces the inversion layer. Another important difference of the GaN HEMT in comparison to a conventional Si MOSFET is the non-doped substrate, which causes in principle a steep subthreshold current characteristics. Regrettably, due to the existence of trap sites at the interfaces of different layers, the subthreshold-current slope is usually degraded from this expected steep characteristics [3].

In spite of the described specific features of a GaN HEMT, compact modeling is normally done utilizing conventional approaches, which ignore the resulting unique potential distribution within the whole GaN HEMT device [4,5]. We have newly developed a more physical compact model by including the above described GaN HEMT features in the solution of the Poisson equation. By considering all possible induced charges, the trapped charge density and the inherent 2DEG charge explicitly within the Poisson equation, observed GaN HEMT characteristics can be well reproduced. This includes accurate reproduction of the current collapse effect, which is a major concern for the design of real application circuits.

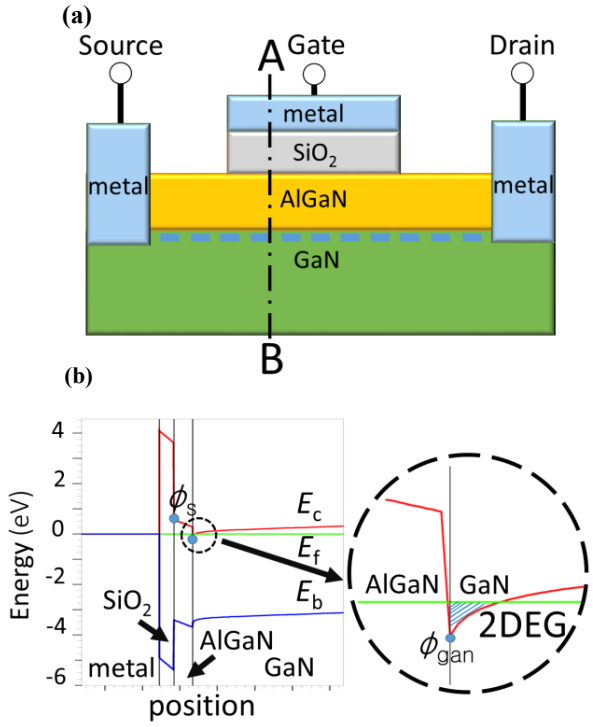

Fig. 1. (a) Studied GaN HEMT structure, (b) Potential distribution along the AB line shown in Fig. 1a.

II. FORMULATION AND SOLUTION OF POISSON'S EQUATION

In our initial considerations, the resistance and the self-heating effects are neglected to concentrate on the novel modeling task for the potential distribution within the device. Fig. 2 depicts the simplified device structure used for the simulation study. 2D device simulation results of potential distributions along the vertical device direction are shown in Fig. 3 for typical gate voltage V_{gs} values at fixed drain voltage V_{ds} of zero. Fig. 4 shows the potential values at three surfaces (see Fig. 1) as a function of the gate voltage V_{gs} for V_{ds}=0V. Around V_{gs}=-15V the inherent 2DEG is formed, and further increase of V_{gs} results in the formation of the strong inversion at the GaN surface. Beyond V_{gs}=0V, the strong inversion condition even at the AlGaN surface is formed. Thus three different operational regions (I, II, and III) can be distinguished as depicted in Fig. 4. The conventional modeling approach, which approximates the inversion charge increase as a function of V_{gs}, is valid only for region II. However, region I is the most trap sensitive part for the long-term device

978-1-4673-7860-4/15/$31.00 ©2015 IEEE

degradation. Region III cannot be ignored as well for optimizing circuit performances by modifying the device structure and bias conditions. Additionally, GaN HEMT is suffering from non-negligible trap effects, and thus the Poisson equation including all possible charges within the device must be considered.

The total charge density within the semiconductor can be written as

$$Q_{gan} + Q_{algan} + Q_{trap} \tag{1}$$

where Q_{gan} and Q_{algan} are charges induced in GaN and AlGaN, respectively. Q_{trap} is the trap density, which is considered to be distributed at the AlGaN/GaN interface with a relatively short time constant for the present study. Since both AlGaN and GaN layers are non-doped, the depletion condition does not occur for the studied device. Within the regions I and II in Fig. 4, Q_{algan} can be ignored and only Q_{gan} together with Q_{trap} exist. Thus the Poisson equation is reduced to a simpler form as

$$\frac{d^2\phi}{dx^2} = -\frac{q}{\varepsilon_{gan}}\left(-n_{gan} - N_t\right) \tag{2}$$

where ε_{gan} is the permittivity of GaN, and n_{gan} and N_t are the carrier density and the trap density in the GaN layer, respectively. Further, n_{gan} in GaN is written as

$$n_{gan} = n_{igan}\exp\left(\beta\phi_{gan}\right) \tag{3}$$

with the intrinsic carrier density n_{igan}. The trap density is

$$N_t = N_0\exp\left(\frac{E_f - E_c}{E_s}\right) \tag{4}$$

$$N_0 = g_c E_s \frac{\frac{kT}{E_s}}{\sin\left(\frac{kT}{E_s}\right)}$$

where β is the inverse of the thermal voltage. The conduction band edge and the Fermi level are denoted by E_c and E_f, respectively, and E_s and g_c are model parameters describing the trap state density. These parameters are extracted with measured *I-V* characteristics. The total charge density within the GaN layer Q_{gan} is written as a function of the surface potential ϕ_{gan} as

$$Q_{gan} = \sqrt{\frac{2q\varepsilon_{gan}n_{igan}}{\beta}}\left\{\exp\left(\beta\phi_{gan}\right) - 1\right\}^{\frac{1}{2}} \tag{5}$$

It is assumed that the carrier trapping occurs at the interface of the AlGaN/GaN interface with a relatively short time constant, and that the trapped carriers are distributed at the interface with the thickness of the inversion layer. The total trap charge density is thus written as

$$Q_{trap} = qN_t \tag{6}$$

The Poisson equation (2) is solved together with the Gauss Law for calculating the potential distribution under applied bias conditions. Here we assume that the AlGaN layer is highly resistive and causes a linearly decreasing potential drop. With this definition, the surface potential ϕ_s is calculated. The boundary condition at the gate oxide and the AlGaN surface is derived under the approximation that the potential drop, induced by creating the inversion charge, is negligible in comparison to that occurring within the non-doped AlGaN layer

$$\frac{V_{gs} - V_{fb} - \phi_s}{T_{ox}}\varepsilon_{ox} = \frac{\phi_s - \phi_{gan}}{T_{algan}}\varepsilon_{algan} \tag{7}$$

In the region III, additional inversion charge Q_{algan} induced at the AlGaN surface must be considered, which is a function of the surface potential ϕ_s and ϕ_{gan}

$$Q_{algan} = \sqrt{\frac{2q\varepsilon_{algan}n_{ialgan}}{\beta}}\left\{\exp\left(\beta\phi_s\right) - \exp\left(\beta\phi_{gan}\right)\right\}^{\frac{1}{2}} \tag{8}$$

where n_{ialgan} is the intrinsic carrier density in the AlGaN layer. The calculation results are depicted together with the 2D simulation results in Figs. 3 and 4. In the Poisson equation, carrier traps are also included to simulate the corresponding effects in a self-consistent way, which result not only in a threshold voltage shift but also in a subthreshold slope degradation as well as a mobility degradation. All these effects are a function of the carrier density.

In addition to the potential-distribution differences there are two further distinguished differences between the GaN HEMT and a conventional MOSFET under normal operating conditions. One is that the 2DEG layer prevents the pinch-off condition and preserves the inversion layer at the GaN surface, as verified in Fig. 5. The other difference is that the Schottky contacts are forcing the consumption of all potential biases applied between source and drain contacts within the semiconductor. These differences of the GaN HEMT can be captured automatically in the compact model by solving the Poisson equation with the Quasi-Fermi level under the gradual channel approximation.

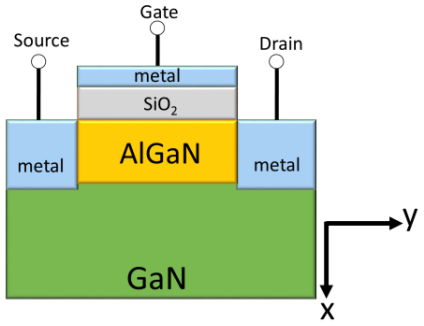

Fig. 2. Simplified GaN HEMT structure studied for the present investigation.

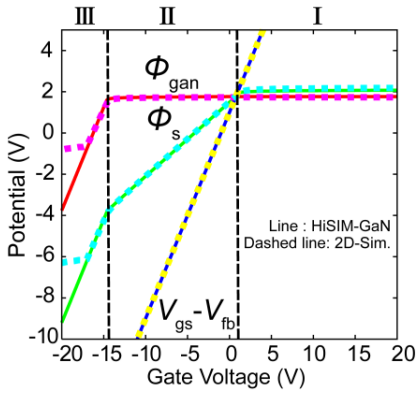

Fig. 3. Two surface potential distributions as a function of V_{gs} (see Fig. 1) and V_{gs}-V_{fb}, where V_{fb} is the flat-band voltage.

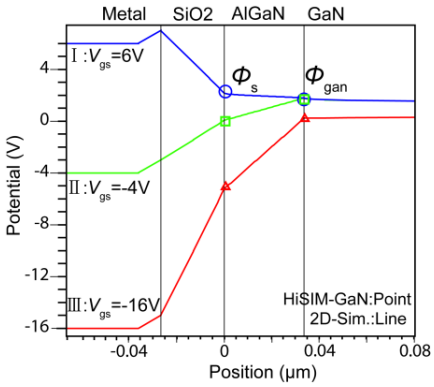

Fig. 4. Potential distribution along the vertical direction for different V_{gs} condition

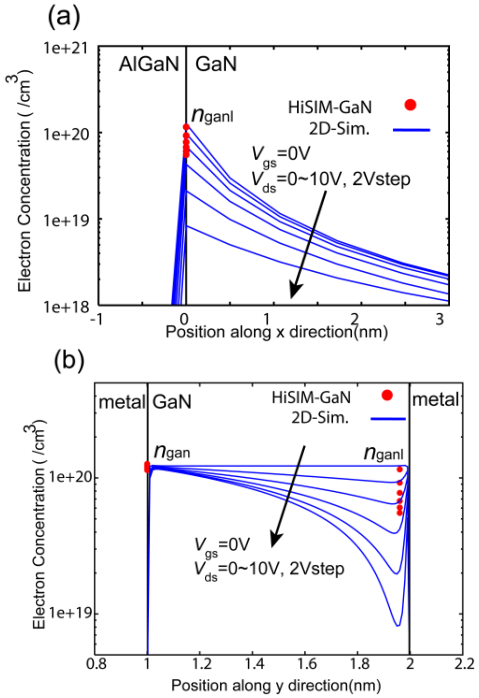

Fig. 5. 2D-device simulation results of electron density distribution (a) vertical to the device surface, and (b) along the lateral direction from source to drain.

III. Comparison with 2D Device Simulation Results

The developed GaN HEMT compact-model equations are added to the industry-standard model HiSIM_HV for power MOSFETs to additionally solve the resistance effect consistently by introduction of internal nodes [6]. HiSIM HV solves the potential distribution along the surface by solving the Poisson equation iteratively. The HiSIM compact model determines the complete potential distribution along the device including the surface potential at the source side ϕ_{s0}, the potential at the pinch-off point ϕ_{sl}, and additionally at the internal node within the resistive drift region [7]. At the drain side, the quasi-Fermi potential is considered for all surface potentials. Fig. 5 includes the calculated surface potential values for different V_{ds} values together with those of the source side.

In the GaN HEMT compact model, the gradual-channel approximation together with approximations of an idealized gate structure are used. Then the equation for the drain current I_{ds} can be written as shown in (9) to (12)

$$I_{ds} = \frac{W_{gate}}{L_{gate}} \mu \frac{I_{dd}}{\beta} \tag{9}$$

$$I_{dd} = (Q_l - Q_0) - \frac{\beta}{2}(Q_l + Q_0)(\phi_{ganl} - \phi_{gan}) \tag{10}$$

$$Q_0 = \sqrt{\frac{2q\varepsilon_{gan} n_{igan}}{\beta}} \left\{ \exp(\beta\phi_{gan}) - 1 \right\}^{\frac{1}{2}} \tag{11}$$

$$Q_l = \sqrt{\frac{2q\varepsilon_{gan} n_{igan}}{\beta}} \left\{ \exp(\beta\phi_{ganl}) - 1 \right\}^{\frac{1}{2}} \tag{12}$$

where W_{gate} and L_{gate} are gate width and gate length, Q_0 and Q_l are the charge densities at source side and drain side, respectively. The carrier mobility μ considers both the low field and high field.

Figs. 6a and b show calculated I_{ds}-V_{gs} results with the developed compact model in comparison to 2D device-simulation results. Fig. 6c shows the respective comparison of the I_{ds}-V_{ds} characteristics, where the current gradually increases even under the saturation condition. The reason is a diminished pinch-off condition due to the existence of the 2DEG. Due to the existence of the AlGaN layer between the gate insulator and the 2DEG of the inversion layer, the gate control is weakened in comparison to the conventional MOSFET. Consequently, no clear conventional mobility universality has been observed.

Fig. 7a demonstrates simulation results with a pulse input with frequency of 10kHz for the circuit shown in Fig. 7b. It is seen that a current reduction occurs after each repetition of the input pulse. This is called the current collapse effect [3]. The reproduction of this observed current collapse effect caused by the gradually increasing trap density is achieved. Due to consideration of the trap charge in the Poisson equation, which is extracted from measured *I-V* characteristics, the current collapse effect is automatically included in the developed GaN HEMT compact model.

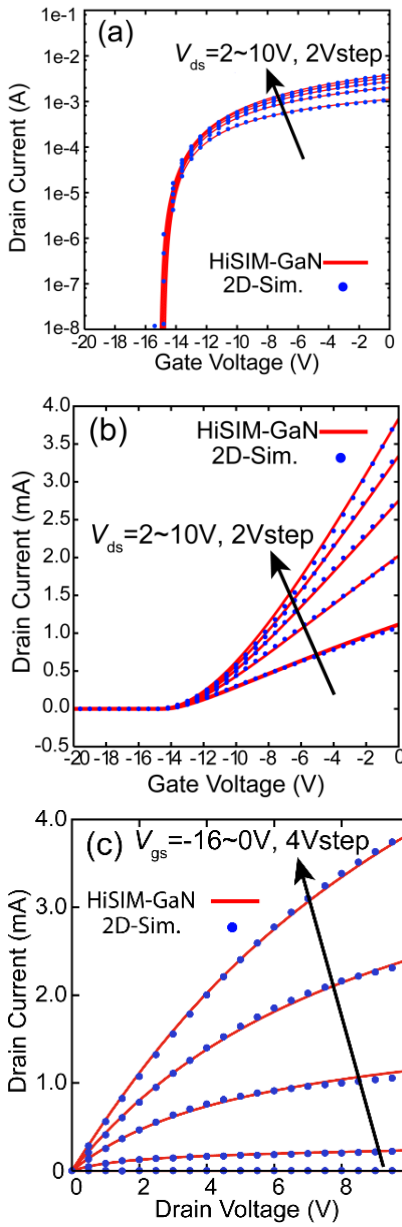

Fig. 6. Comparison of model results to 2D-device simulation results for different bias conditions. (a) logI_{ds}-V_{gs}, (b) I_{ds}-V_{gs}, (c) I_{ds}-V_{ds}.

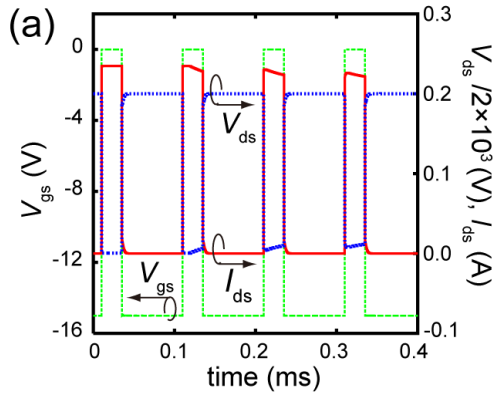

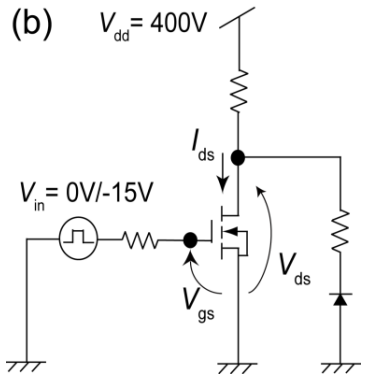

Fig. 7. (a) Calculated transient characteristics with the circuit shown in (b). Continuous trap density increase causes the observed current collapse

IV. CONCLUSION

The reported GaN HEMT compact model is based on a complete surface-potential description, which considers all induced charges and in addition the trap density at the AlGaN/GaN interface. It is verified that the developed model can reproduce all observed DC as well as transient GaN HEMT characteristics automatically.

REFERENCES

[1] M. A. Khan, A. Bhattarai, J. N. Kuznia and D. T. Olson, "High electron mobility transistor based on a GaN-AlxGa1-xN heterojunction," Appl. Phys. Lett., vol.63, no. 9, pp.1214-1215, Aug. 1993.

[2] W. Saito, M. Kuraguchi, Y. Takada, K. Tsuda, T. Domon, I. Omura, and M. Yamaguchi, "380 V/1.9A GaN power-HEMT: Current collapse phenomena under high applied voltage and demonstration of 27.1 MHz class-E amplifier," IEDM Tech. Dig., pp. 597-600, 2005.

[3] G. Longobardi, F. Udrea, S. Sque, J. Croon, F. Hurkx, J. Sonsky, "The dynamics of surface donor traps in AlGaN/GaN MISFETs using transient measurements and TCAD modelling," IEDM Tech. Dig., p430, 2014.

[4] I. Angelov, K. Andersson, D. Schreuers, N. Rorsman, V. Desmaris, M. Sudow, H. Zirath "Large-signal modeling and comparison of AlGaN/GaN HEMTs and SiC MESFETs," Proc. APM, 2006.

[5] U. Radhakrishna, D. Piedra, Z. Yuhao, T. Palacios, D. Antoniadis, "High voltage GaN HEMT compact model: Experimental verification, field plate optimization and charge trapping," IEDM Tech. Dig., pp.32.7.1-32.7.4, Dec. 2013.

[6] H. J. Mattausch, M. Miyake, T. Iizuka, H. Kikuchihara, M. Miura-Mattausch, "The Second-Generation of HiSIM_HV Compact Models for High-Voltage MOSFETs," IEEE TED, pp. 653-661, Jan. 2013.

[7] M. Miura-Mattausch, H. J. Mattausch, T. Ezaki, "The Physics and Modeling of MOSFETs," World Scientific, 2008.